

Tailoring of the Porosity in Sol-Gel Derived Silica Thin Layers[†]

M. Klotz, A. Ayrat, C. Guizard, and L. Cot*

Laboratoire des Matériaux et Procédés Membranaires, UMR5635 CNRS - ENSCM - UMII
ENSC Montpellier- 8, rue de l'École Normale F34296 Montpellier cedex 5, France

Received March 27, 1999

The sol-gel process enables the preparation of ceramic thin films ranging in characteristics from dense to highly porous layers. Based on the example of silica layers, this paper focuses on the importance of the choice of the various synthesis parameters to tailor the porosity of the final material and new opportunities associated to the templating effect. The problems related to the characterization of the porosity in the case of thin films are also considered.

Introduction

The sol-gel route is a very convenient method to prepare porous thin layers of ceramic oxides. Fluid starting sols can be deposited on dense or porous substrates leading to defect free submicrometer thin films.¹ The porosity in the final layers however, depends greatly on the various synthesis parameters. The requirements associated with the final application of the thin layers allow for the definition of an ideal porosity in terms of total porosity, pore size, pore size distribution, connectivity and tortuosity of the porous network. The preparation of silica thin layers is chosen as an example of the various synthesis strategies available to tailor the final porosity. The problem of the characterization of the porosity of the thin layers is also introduced in the last part of this paper.

Sol-gel Routes and Elemental Bricks

The initial choice is related to the nature of the precursor of the inorganic network. Two main types of sol-gel routes can be distinguished. In the polymeric route the elemental unit that is initially used is a molecular precursor, usually a metal-organic compound of alkoxide type $M(OR)_n$. For silica, the most common precursors are tetramethoxysilane $Si(OCH_3)_4$ (TMOS) and tetraethoxysilane $Si(OC_2H_5)_4$ (TEOS) in solution in their associated alcohols. In the colloidal route, the elemental unit is a solid nanoparticle dispersed as stable sol in a liquid. The sol stability is related to electrostatic and steric repulsive interactions. Various silica hydrosols are commercially available with particle size ranging from 10 nm to 40 nm.

These elemental units are the bricks from which is built the oxide network. The choice of the size of the brick will first define the size of the pores in the layer. For spheres with a single particle size (radius R), an ordered close-packed arrangement (face-centred cubic or hexagonal) gives rise to

a porosity of 26% and to two types of pores with a radius equal to $0.225 R$ (tetrahedral sites) and $0.414 R$ (octahedral sites), respectively. For a dense random packed arrangement, the lowest limit for the porosity is 36%, with a pore size distribution ranging from $0.2 R^2$ to $0.6 R^2$. In the case of a distribution of particle sizes, denser packing can be obtained,³ and the pore size distribution depends strongly on the composition of the mixture of spheres (Figure 1).⁴

From this first set of data it appears clearly that the preparation of mesoporous layers (pore size between 2 nm and 50 nm) can be considered using colloidal dispersions. For the preparation of microporous layers (pore size less than 2 nm), the most convenient way is the polymeric route from solutions of molecular precursors, like alkoxides.

Aggregation and Polymerization

Gelation of colloidal dispersions. In order to obtain the formation of the solid network the aggregation of the colloidal particles must be promoted. In the case of the preparation of thin films, the starting sols are only very slightly aggregated if at all. The evaporation of the liquid phase during the drying of the layers causes the colloidal particles to aggre-

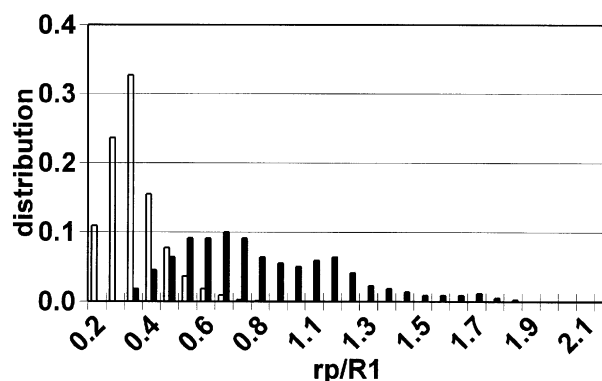


Figure 1. Pore size distribution for two dense random packed arrangements produced from a bimodal mixture of small spheres (radius R_1) and large spheres (radius $R_2 = 4 R_1$) and exhibiting the same total porosity (30%); black bars: 10% of small spheres; white bars: 75% of small spheres (from ref. 4).

[†]Basis of the presentation given at International Joint Seminar on New Trends in Material Chemistry 12-13 March 1999, Seoul National University, Seoul, Korea

Table 1. pH effect on the porous texture of colloidal silica gels produced by evaporation of the aqueous phase (particle diameter = 12 nm)

pH	sol stability	porosity (%)	average pore diameter (nm)
2	+	47	7
6	-	54	10
10	++	32	4

gate and form a continuous network. The stability of the starting sol determines the gelation volume and, as a consequence, the density of the final arrangement: the more stable the sol, the denser the layer. The effect of the stability of a quasi-monodispersed silica sol on the porosity and on the pore size of the final material is shown in Table 1.

Gelation of alkoxide solutions. The formation of the oxide network is a result, in this case, of the polymerization of the molecular precursor. The hydrolysis of the alkoxide (a) produces activated species and the condensation by alcoxolation (b) or oxolation (c) leads to a reticulation by formation of siloxane bridges =Si-O-Si=.



Looking more closely at the silicon alkoxides, the hydrolysis and condensation reactions are catalysed in acid and base media, respectively. The polymerization process is modified as a function of the synthesis conditions. Acid catalysis promotes the formation of linear polymers and long gelation times t_G . The formation of dense clusters and short gelation times t_G are favoured by base catalysis. The hydrolysis ratio (water : alkoxide molar ratio) is another important parameter. For a given alkoxide, differences in the synthesis conditions give rise to important differences in the porous texture of the final material as shown in Tables 2 and 3.

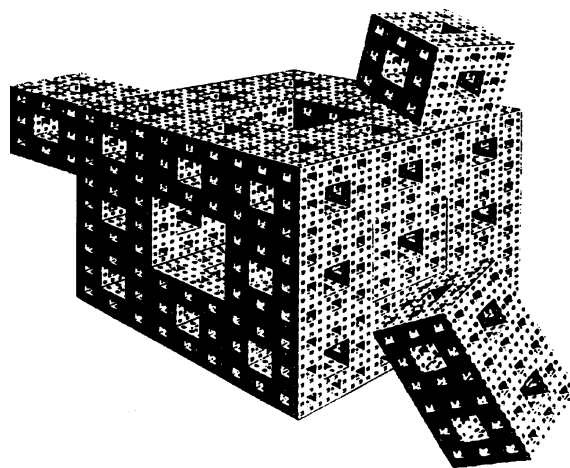
Gelation mechanisms. The nature of the solid network

Table 2. Influence of the hydrolysis method on the porous texture of polymeric silica gels synthesised using TEOS (from ref. 1)

hydrolysis	porosity (%)	pore diameter (nm)	specific surface area (m ² /g)
two-step acid-catalysed	54	1-5	740
two-step acid-base-catalysed	67	1-10	910
one-step base-catalysed	70	1-20	515

Table 3. Textural characteristics determined by thermoporometry on wet and dried silica gels prepared with various hydrolysis ratio h (molar ratio eau/TEOS) (from ref. 5)

h	porosity (%)		average pore diameter (nm)		specific surface area (m ² /g)	
	wet	dried	wet	dried	wet	dried
4	78	42	7	6.5	1012	296
6	78	42	9	6.5	720	337
10	82	47	10	6	812	518
15	77	45	11	5	618	452

**Figure 2.** Schematic representation of the aggregation of fractal clusters using Menger sponges (the elemental brick is a cube) (from ref. 6).

generated by aggregation of colloids or polymerization of alkoxides depends on the diffusion of the elemental species and of the growing clusters (effects of dilution, viscosity, temperature). It depends also on the probability of aggregation during a contact between two species (reactivity). Various models were proposed that are associated with a limiting mechanism for the growth: diffusion-limited monomer-cluster or cluster-cluster growth, reaction-limited monomer-cluster or cluster-cluster growth. The resulting clusters or aggregates usually exhibit a fractal (or hierarchical) structure for scales above that of the elemental unit size. By this route the gelation process leads to a large size distribution for the intra and inter-cluster pores as schematically illustrated on Figure 2.

Drying of the layers. In the case of thin layers, the deposition is carried out with a fluid sol before the gelation (at $t < t_G$). The reticulation occurs simultaneously with the drying of the layer, which induces a concentration of the sol. The final porous texture is strongly dependant on the relative kinetics of polymerization and solvent evaporation.

Aging of the sols. An important parameter is the aging of the sol before deposition. This parameter defines the advancement of the polymerization process before the deposition of the sol and, consequently, the porous texture of the resulting layer (Table 4).

Aging of the wet gels. The porosity of the wet gels is filled by the liquid phase. With the evaporation of the liquid,

Table 4. Ageing of polymeric silica sols prior to film deposition; effect on the porous texture of the resulting layers (from ref. 7)

ageing before deposition t/t_g	porosity (%)	average pore diameter (nm)	specific surface area (m ² /g)
0-0.15	-	< 0.4	1-2
0.15	16	3.0	146
0.33	24	3.2	220
0.66	33	3.8	263
1	52	6.0	245

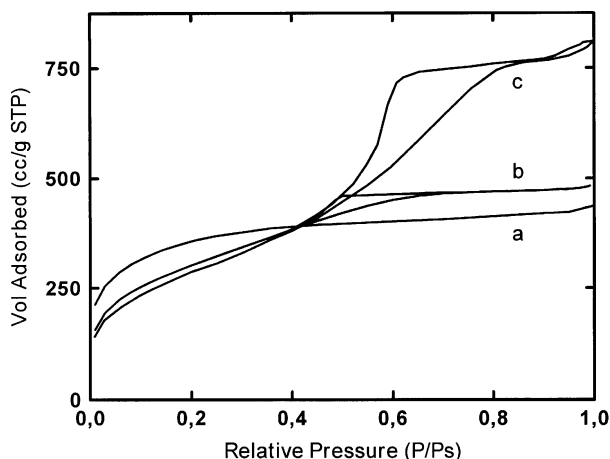


Figure 3. Nitrogen adsorption-desorption isotherms for the samples a, b, c described in Table 5.

menisci appear in the pores and capillary stresses are applied on the solid network, which shrinks. The porous texture is strongly modified by the drying step (Table 3). The monolithic structure of the bulk gels is usually not preserved as cracking occurs. Concerning the sol-gel layers, films thinner than $0.5 \mu\text{m}$ can be dried without cracking, whereas for a thickness greater than $1 \mu\text{m}$, cracking is usually observed.¹

Evaporation can be reduced or stopped during and after the deposition in order to promote reinforcement of the inorganic network before the drying stage. Figure 3 and Table 5 illustrate the effect of wet gel aging on the porous texture of the final material. The studied materials show two length levels of porosity: microporosity within the polymeric silica clusters and mesoporosity between clusters as is usually observed in the case of two-step acid-base-catalyzed silica gels. The aging enables the maintainance of a high porous volume in the dried gel, which is essentially associated with the large inter-cluster mesoporosity initially present in the wet gel.

A possible way to avoid capillary stresses is to carry out supercritical drying by removing the liquid above the critical temperature and pressure of the solvent.¹ This drying method, however, cannot be easily adapted to the case of thin layers. Another strategy consists of the insertion of removable entities in to the wet gel network, which help support the capillary stresses during the drying stage and which can be eliminated by thermal or chemical treatment after the reinforcement of the solid network. Moreover, these entities act as templates, generating a porosity of the same shape and size as the templating units.

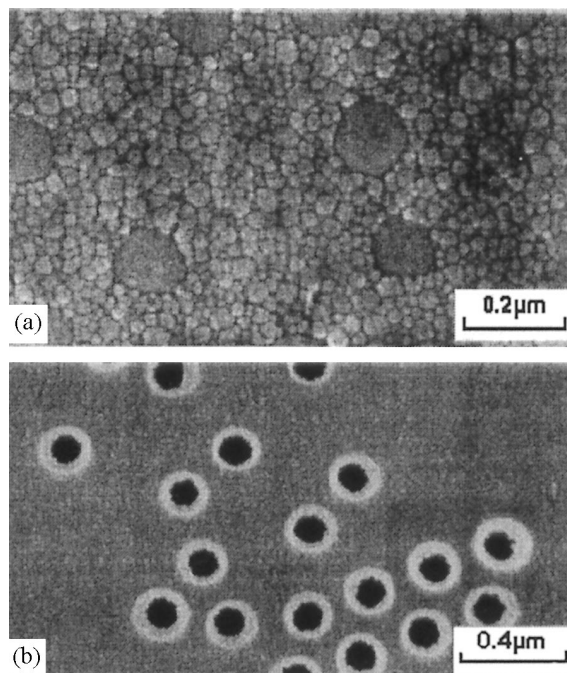


Figure 4. Scanning electron microscopy observation on thin films prepared from mixtures of silica colloidal particles and polystyrene latex. (a) untreated layer; (b) layer treated at $250 \text{ }^\circ\text{C}$ (disappearance of the polystyrene spheres and production of spherical pores).

Tailoring of the Porosity by Templating Effects

Use of individual particles as templates. The templating entities can be individual species ranging in size from small molecules to solid particles. This last case is illustrated in Figure 4. In this example, hybrid dispersions based on colloidal silica - polystyrene latex mixtures are used to prepare macroporous silica thin films with spherical pores.⁸

Use of interconnected and ordered networks as templates. In addition to controlling pore size and pore volume, it is also particularly interesting to control the connectivity of the porosity and the permeability of the porous material. K. Nakanishi *et al.*⁹ used the spinodal decomposition of sol-gel solutions into two phases, one rich in solvent and the other rich in polyethylene oxide and inorganic compounds, to produce dried gels with interconnected porosity in the micrometer range. Unfortunately this method cannot be extended to the nanometer range. Another strategy to produce an interconnected porosity is the templating route. But in that case the individual templating units have to be replaced by removable interconnected networks.

At the nanometer scale the lyotropic liquid crystal

Table 5. Effect of ageing prior to drying for wet silica gels synthesised by two-step acid-base hydrolysis of TMOS

sample	ageing	pore volume ($\text{cm}^3 \cdot \text{g}^{-1}$)	porosity (%)	μ -porosity (% of porosity)	specific surface area (m^2/g)
a	dried after deposition at $t \sim 0.05 t_G$	0.68	60	86	1264
b	dried immediately after the gelation	0.74	62	72	1106
c	dried after 3 days of ageing at $50 \text{ }^\circ\text{C}$	1.23	73	42	1056

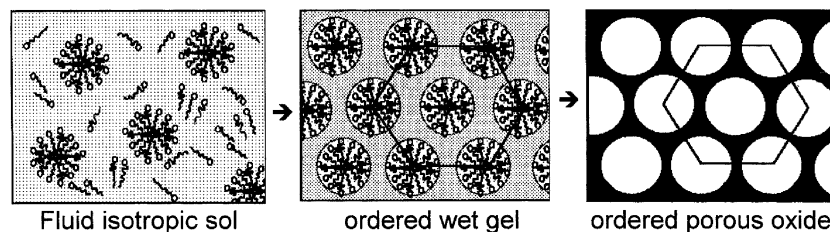


Figure 5. Schematic representation of the sol-gel processing using a hexagonal mesophase as structure directing template.

mesophases, which are obtained by a self-assembly process of surfactant molecules, appear as very attractive systems. Moreover, the crystalline structure of these templates orients the growth of the inorganic network and leads to the formation of ordered structure and porosity. The periodicity of the structures involves the pore size monodispersity and defines a uniform connectivity of the porous and solid networks. The main lyotropic liquid crystals are lamellar (surfactant bilayers separated by aqueous layers), hexagonal (hexagonal arrangement of cylindrical micelles) and intermediate cubic structures.

In 1992 researchers at Mobil published a synthesis method of mesoporous molecular sieves using the templating effect of lyotropic liquid crystal mesophases.^{10,11} The aluminosilicate or silicate materials labelled M41S, are prepared by hydrothermal treatment of solid or molecular inorganic precursors in the presence of cationic surfactants of alkyl trimethyl ammonium halogenide type, $C_xH_{2x+1}(CH_3)_3N^+, X^-$. As a matter of fact, various studies show that the synthesis of silica network in ordered amphiphilic media can also be obtained by sol-gel routes at room temperature and atmospheric pressure. Others types of surfactant, anionic or non-ionic, can also be used. In different processes, phase separations occur in the synthesis solutions. In other cases, extraposity is observed on a larger scale than the ordered porosity produced by the templating mesophases.^{12,13}

Our approach for the sol-gel synthesis of these kinds of porous solids was based on the required properties of the final material: a continuous thin layer with a porosity limited to the ordered porosity generated by the crystalline template. The synthesis method is schematically represented in Figure 5. TMOS was mixed with an aqueous solution of cationic surfactant of alkyl trimethyl ammonium bromide type: $C_xH_{2x+1}(CH_3)_3N^+, Br^-$ ($x = 8, 10, 12, 14, 16$).¹⁴⁻¹⁶ The thermal elimination of the template was obtained after a thermal

Table 6. Textural properties of hexagonal silica gels determined from nitrogen adsorption measurements or calculated from the structural data. (x , number of carbons of the alkyl chain of the surfactant; a , cell parameter of the hexagonal lattice; d_c , calculated diameter of the cylindrical pores of a hexagonal structure, d_p , measured average pore diameter; S_c and S_m , calculated and measured specific surface areas)

x	a (nm)	d_c (nm)	d_p (nm)	S_c (m ² /g)	S_m (m ² /g)	porosity (%)	μ -porosity (% of P)
8	2.7	2.1	1.9	1074	1260	60	82
10	3.2	2.5	2.3	883	1040	57	88

treatment up to 450 °C. Continuous thin layers were deposited on porous ceramic substrates and tested as separate membranes.¹⁷ Hexagonal phases and associated ordered porous materials were initially limited to the lower values of x : 8 and 10.¹⁶ Table 6 shows that the pore size can be modulated by the length of the alkyl chain of the surfactant and that there is good agreement between the textural characteristics calculated from the structural data and that determined from nitrogen adsorption measurements. The preparation of hexagonal phases and resulting porous layers were recently extended to the full range of x values (Figure 6).¹⁸

An important aspect concerns the anisotropy of the ordered domains in the case of layers. Interactions at the gel-substrate and air-gel interfaces favor the preferential orientation of the hexagonal and lamellar structures along these

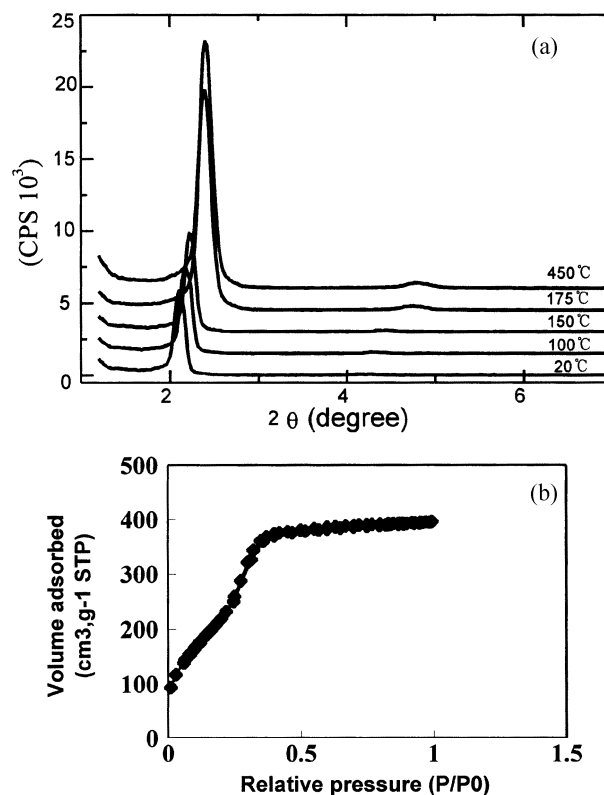


Figure 6. Thin layer synthesised using TMOS and hexadecyltrimethylammonium ($x=16$). (a) X ray patterns obtained after thermal treatment at various temperatures. The main diffraction peak is assigned to the Bragg spacing d_{100} of a hexagonal phase. (b) nitrogen adsorption-desorption isotherm for the layer thermally treated at 450 °C.

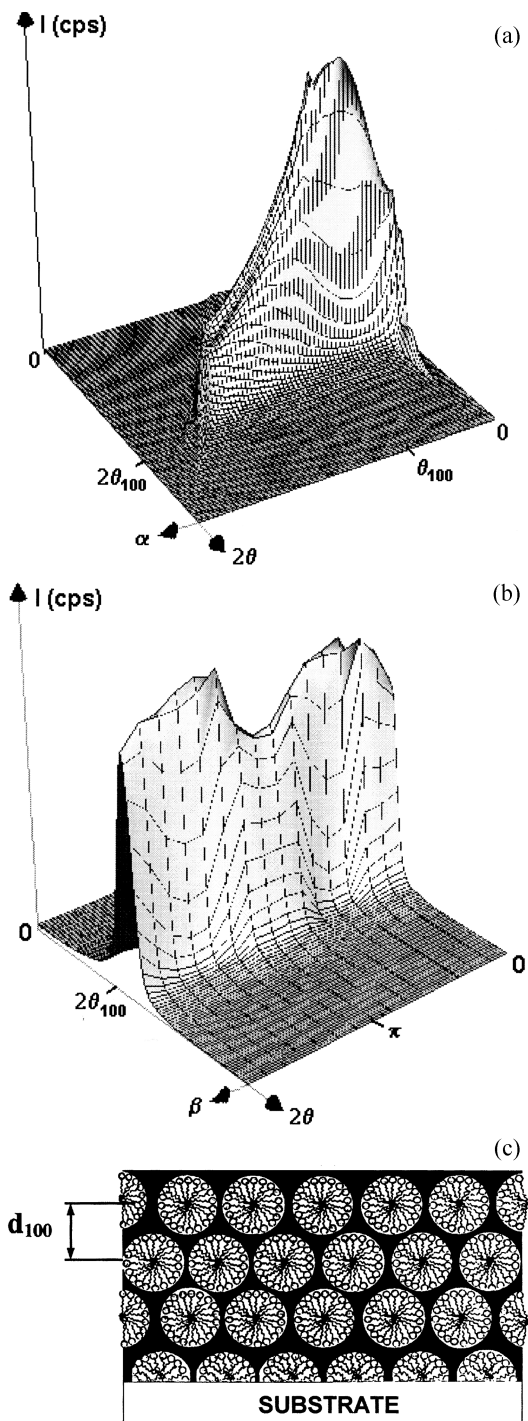


Figure 7. X ray diffraction study of the anisotropy of a thin layer thermally treated at 450 °C: variation of the intensity of the d_{100} peak: (a) versus α , angle between the incidence beam and the layer plane; (b) versus β , angle between the projection of the incidence beam on the layer plane and the direction of withdrawal during the deposition. (c) schematic representation of the alignment of the micellar cylinder parallel to the substrate plane in an untreated thin layer - case of a hydrophobic substrate (from ref. 21).

interfaces.¹⁹⁻²² Moreover, shear stresses applied during the deposition can induce an alignment of the crystalline structures in the direction of the stresses. X ray analyses enable us to evidence these anisotropies (Figure 7). To improve the

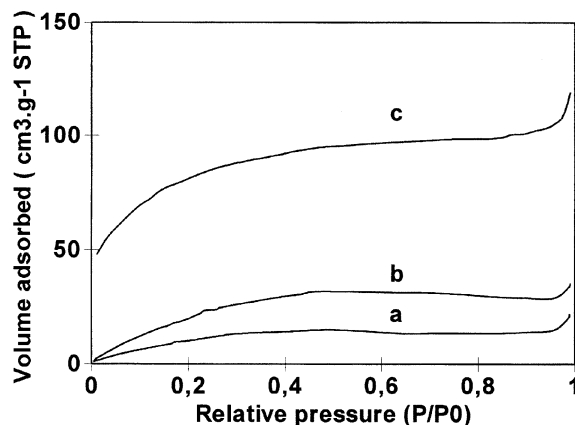


Figure 8. Nitrogen adsorption isotherms for microporous supported thin layers produced from sols based on TEOS (a, b) or a TEOS - methyl triethoxysilane mixture (c) and deposited at $t < 0.01 t_G$.

permeability of the final porous layers it seems interesting to orient the templating structures, and as a result, the resulting pores along a direction perpendicular to the layer surface. Based on previous results on ferromagnetics,²³ our approach to improve the texture consists of the introduction of magnetic nanoparticles in the gelling solution. First experiments and X rays analyses showed the positive seeding effect on the texture of the wet gels.²⁴

Characterization of the Porosity of Thin Layers

The characterization of the porosity of thin films is a complex problem if, beyond the total porosity, the pore size and the pore size distribution are analysed. The methods based on gas adsorption are the most convenient for the study of microporous and mesoporous materials. The conventional equipment employs volumetric measurements of the adsorbed gas quantities.²⁵ Unfortunately in the case of thin films deposited on a substrate, the amount of porous layer that can be introduced in a standard-size sample cell is too small to be correctly characterized. Other types of adsorption equipment were developed, like the surface acoustic wave device²⁶ or a device based on the measurement of the refractive index by ellipsometry.²⁷ These techniques, however, require specific conditions concerning the nature of the substrate. In the first case, the substrate must be piezoelectric, while in the second case, the layer must be transparent and the refractive index of the substrate must be quite different from that of the layer. Each substrate exhibits specific surface properties that can have an influence on the final characteristics of the deposited coatings. In order to study the layers on their own substrate, we tried to conciliate the conditions of use for a conventional adsorption apparatus with the specificities associated with thin layers. The volume of the sample cell was increased and the free volume was minimized.²⁸

Using this method, we studied the porosity of poorly porous sol-gel derived silica thin layers deposited on soda-lime-silica glass and we compared their characteristics with

Table 7. Variation of the porous texture between thin films and corresponding thick layers (sols 1 and 2 were prepared by one-step base hydrolysis of TEOS and deposited at $t < 0.01 t_G$)

sol - layer	pore volume (cm ³ /g)	porosity (%)	specific surface area (m ² /g)
1 - thin	0.01	2.4	30
1 - thick	1.10 ⁻⁴	<0.1%	<0.5
2 - thin	0.02	4.3	52
2 - thick	5.10 ⁻⁵	<0.1%	<0.2

that of self-supported cracked thick layers obtained from the same gelling solutions. The adsorption curves (Figure 8) for the supported thin layers correspond to type I isotherms²⁵ associated with mainly microporous materials as expected in the case of an acidic hydrolysis. From the results reported in Table 7, it is also possible to compare the porosity of the thin coatings and that of the corresponding cracked thick layers. The thick layers appear as dense material when using nitrogen adsorption measurements. This difference shows the effect of the substrate during the drying of the supported thin layers. It opposes the shrinkage of the coating, leading to a higher porosity in the layer. These results underscore also the importance of the characterization of the layers on their own substrate.

Conclusion

As a function of the requirements associated with its application, the porosity of a sol-gel derived layer can be tailored by means of a strict control of the synthesis parameters during the successive preparation steps. New and attractive opportunities exist to improve the porosity by using the templating effect of individual particles or interconnected networks. The improvement of the characterization methods must also contribute to the optimization of the synthesis conditions to prepare better layers.

References

1. Brinker, C. J.; Scherer, G. W. In *Sol-gel science, the physics and chemistry of sol-gel processing*; Academic Press: Boston, 1990.
2. Frost, H. J.; Raj, R. *J. Am. Ceram. Soc.* **1982**, *65*, C19.
3. Ben Aim, R. *Thesis*, University of Nancy (France) 1970.
4. Troadec, J. P.; Bideau, D. In Proceedings of *Journal sur la préparation, la caractérisation et la manipulation des poudres céramiques*, Paris (France), 12 February 1992; Groupe Français de la Céramique, Paris, 1992; p 33.
5. Quinson, J. F. In Proceedings *Ecole d'é Procédés sol-gel*, Bombannes (France), 28 September-2 October 1987; CNRS, Paris, 1987; Vol. II, p 10.
6. Zarzycki, J. In *Science of Ceramic Chemical Processing*, Hench, L.L. and Ulrich, D.R. Eds.; Wiley: New York, 1986; p 21.
7. Brinker, C. J.; Frye, G. C.; Hurd, A. J.; Ashley C. S. *Thin Solid Films* **1991**, *201*, 97.
8. Ayral, A.; Guizard, C.; Cot, L. *J. of Materials Sc. Letters* **1994**, *13*, 1538.
9. Nakanishi, K.; Yamasaki, Y.; Kaji, H.; Soga, N.; Inoue, T.; Nemoto, N. *J. Sol-Gel Sci. and Technol.* **1994**, *2*, 227.
10. Kresge, C. T.; Leonowicz, M. E.; Roth, W. J.; Vartuli, J. C.; Beck, J. S. *Nature* **1992**, *359*, 710.
11. Beck, J. S.; Vartuli, J. C.; Roth, W. J.; Leonowicz, M. E.; Kresge, C. T.; Schmitt, K. D.; Chu, C. T. W.; Olson, D. H.; Sheppard, E. W.; McCullen, S. B.; Higgins, J. B.; Schenker, J. L. *J. Am. Chem. Soc.* **1992**, *114*, 10834.
12. Martin, J. E.; Anderson, M. T.; Odinek, J.; Newcomer, P. *Langmuir* **1997**, *13*, 4133.
13. Anderson, M. T.; Martin, J. E.; Odinek, J.; Newcomer, P.; Wilcoxon, J. P. *Microporous materials* **1997**, *10*, 13.
14. Dabadie, T. *Thesis*, University of Montpellier (France): 1994.
15. Dabadie, T.; Ayral, A.; Guizard, C.; Cot, L.; Robert, J. C.; Poncelet, O. *Mat. Res. Soc. Symp. Proc.* **1994**, *346*, 849.
16. Dabadie, T.; Ayral, A.; Guizard, C.; Cot, L.; Lacan, P. *J. Mat. Chem.* **1996**, *6*, 1789.
17. Dabadie, T.; Ayral, A.; Guizard, C.; Cot, L.; Robert, J. C.; Poncelet, O. In *Proceedings of the Third International Conference on Inorganic Membranes*, July 1994, Worcester (USA) Ma, Y. H. Ed.; Worcester Polytechnic Institute, Worcester, 1994; p 411.
18. Klotz, M.; Ayral, A.; Guizard, C.; Cot, L. to be published.
19. Yang, H.; Kuperman, A.; Coombs, N.; Mamiche-Afara, S.; Ozin, G. A. *Nature* **1996**, *379*, 703.
20. Yang, H.; Coombs, N.; Sokolov, I.; Ozin, G. A. *Nature* **1996**, *381*, 589.
21. Yang, H.; Coombs, N.; Sokolov, I.; Ozin, G. A. *J. Mat. Chem.* **1997**, *7*, 1285.
22. Raimondi, M. E.; Maschmeyer, T.; Templar, R. H.; Seddon, J. M. *Chem. Commun.* **1997**, 1843.
23. Fabre, P.; Casagrande, C.; Veyssie, M.; Cabuil, V.; Massart, R. *Phys. Rev. Letters* **1990**, *64*, 539.
24. Klotz, M.; Ayral, A.; Van der Lee, A.; Guizard, C.; Menager, C.; Cabuil, V. to be published in *Mat. Res. Soc. Symp. Proc.* 1998, vol. 519.
25. Lowell, S.; Shields, J. E. In *Powder surface area and porosity*, Chapman and Hall, London, 1984.
26. Frye, G. C.; Ricco, A. J.; Martin, S. J.; Brinker, C. *J. Mat. Res. Soc. Symp. Proc.* **1988**, *121*, 349.
27. Fardad, M. A.; Yeatman, E. M.; Dawnay, E. J. C.; Green, M.; Horowitz, F. *J. Non Cryst. Solids* **1995**, *183*, 260.
28. Ayral, A.; El Mansouri, A.; Vieira, M. P.; Pilon, C. *J. Mat. Sc. Letters* **1998**, *17*, 883.